Design and Verification of Smart and Scalable DC Microgrids for Emerging Regions

P. Achintya Madduri, Javier Rosa, Seth R. Sanders, Eric A. Brewer, and Matthew Podolsky
Department of Electrical Engineering and Computer Science
University of California, Berkeley
Berkeley, USA

Abstract—**Roughly 1.3 billion people in developing countries still live without access to reliable electricity. As expanding access using current technologies will accelerate global climate change, there is a strong need for novel solutions that displace fossil fuels and are financially viable for developing regions. A novel DC microgrid solution that is geared at maximizing efficiency and reducing system installation cost is described in this paper. Relevant simulation and experimental results, as well as a proposal for undertaking field-testing of the technical and economic viability of the microgrid system are presented.**

I. INTRODUCTION

Millions of unelectrified households in rural developing regions rely on fossil fuels (mainly kerosene) for their primary lighting needs; fossil fuels are an inefficient source of lighting and their use represents a large negative environmental and health impact. Most of these unelectrified households are located in villages and hamlets that are predominantly unconnected to the central electricity grid. These households will drive most of the medium-term growth in energy consumption [1]. Grid extension to meet their energy needs is not viable because of the high connection costs faced by households and disincentives for grid operators to provide connectivity stemming from high transmission losses and theft [2]. Furthermore, studies show that grid extension does not guarantee access to electricity: there is a high degree of load-shedding, and service reliability is weak for rural customers [3]. However, the falling cost of solar panels and batteries provides for a viable renewable alternative to grid-generated electricity. Based on the usage data from recent field studies to establish central inverter-tied conventional AC microgrids [4] there is a strong body of evidence to suggest that a fully DC system with distributed storage at every household will increase the efficiency and reduce the costs of providing sustainable, reliable electricity to rural developing regions.

A DC village-microgrid (Figure 1) with the goal of meeting the dynamic electricity needs of households within a 2 km radius will integrate the following features:

1) DC power generation and distribution: Line transmission losses will be minimized by using 380 VDC and converted to safer 12 VDC at the households.
2) Household Power Management Units (PMUs): The DC transmission lines will be connected to each household via a PMU that provides the power for all household appliances. PMUs also integrate scalable distributed
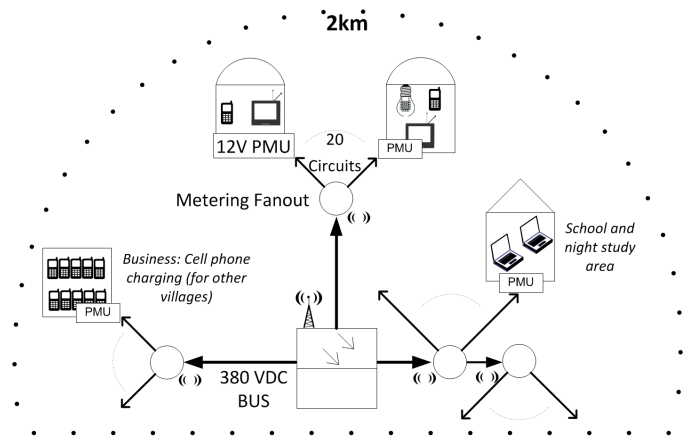

Figure 1. Architectural overview of a DC village-microgrid with a 380VDC transmission bus that is converted to 12VDC for household usage.

storage that is owned by individual households. In addition, the PMUs can digitally communicate information such as price, charge-state of households, credits, and usage to the power station over the power lines.

3) Distributed control scheme to mitigate variability in grid power: A droop voltage power-sharing scheme is implemented, wherein the microgrid voltage droops in response to low-supply/high-demand. The PMUs in turn respond by reducing the power that they are drawing from the grid by using more of the locally stored supply. The control of grid voltage is thereby distributed to the PMUs connected to the grid. This feature is enabled by the combination of DC voltage transmission and distributed storage. Since the PMUs will be able to communicate digitally to the power station, we will also be able to do more advanced scheduling and load-management.

4) High-efficiency DC Appliances: PMUs will have efficient DC-DC converters that provide power to efficient DC appliances (such as LED lighting). Small-scale point-of-load inverters are used for AC devices.

5) Scalable Distributed Storage: Lithium-based storage integrated into individual PMUs will reduce losses of stored energy by minimizing conversion steps and line losses. Distributed storage also allows for household loads to be decoupled from the grid supply as required.

Furthermore, household ownership of batteries allows for flexible, demand-driven growth of storage in the grid; each household makes decisions about the size of their stored supply based on desired night-time usage.

II. MOTIVATION FOR DC MICROGRID SOLUTION

The efficiency gains associated with using a DC architecture for household settings has been explored in the context of integrating renewable resources and electric vehicles in countries with a strong central grid architecture [5], [6]. However the case for deploying DC microgrids in rural developing regions is even stronger due to the combination of the easily available solar resource, which makes using solar generation very viable, and the predominant usage—lighting, cell phone charging, fans—from DC appliances. Studies suggest that a 20% cost-reduction is possible through gains associated with improved power-conversion efficiencies that can be realized with a fully DC microgrid [7], (Table I). Distributed point-of-load converters can achieve higher efficiencies since they can be selectively turned off, and thereby reduce standby losses in the grid.

Figure 2. Overview of the key components of the DC village-microgrid system and their functional blocks.

Factors	AC microgrid system with centralized storage	DC microgrid system with distributed storage
Sizing Issues	Hard to incrementally resize. Inverter losses can dominate with mismatch to load	Lack of inverter/central-storage makes it easy to incrementally add more generation
DC-AC/DC-DC conversion losses	30% [8], [9]: due to central battery bank + inverter	10% daytime, 23% nighttime: due to 3 DC-DC conversion steps [8]
Losses due to internal rectification and conversion in loads	> 25% [10]	0% for DC and >25% for AC loads [10]
End-to-end Efficiency	< 60%	85-77% for DC loads, < 63% for AC loads

Table I
A COMPARISON OF THE IMPORTANT FACTORS RELATING TO USING A CONVENTIONAL AC MICROGRID VERSUS A DC MICROGRID WITH DISTRIBUTED STORAGE.

III. SYSTEM DESCRIPTION/OVERVIEW

An overview of the proposed village microgrid system is shown in Figure 2. The key components of the system are the source converter, fanout nodes, and the home PMUs. The source converter is responsible for operating the solar panels at their peak-power point as well as detecting and dealing with faults on the grid. The grid voltage is allowed to operate between 360-400 VDC and overcurrent and overvoltage protection are integrated into the functionality of the source converter. The fanout nodes are responsible for aggregating usage from a local cluster of houses and for switching and metering of the usage to individual household connected to
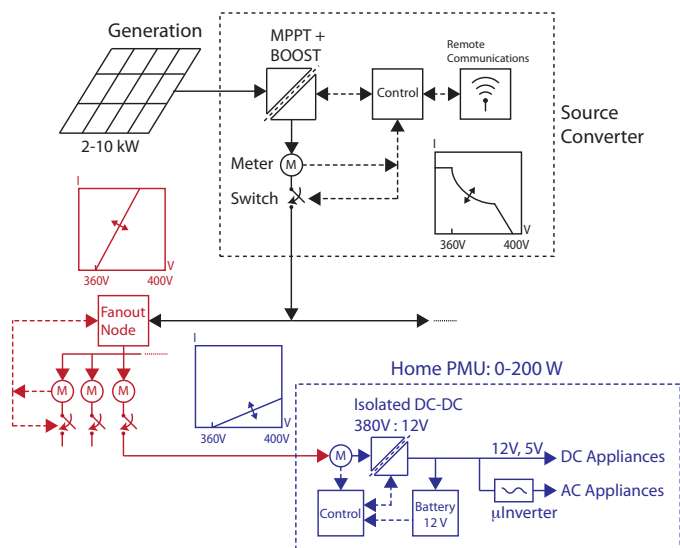
the line; this functionality helps in deterring theft of power as well as isolating faults on the grid. Finally, the PMUs are responsible for distributed control of grid voltage and for providing power for the household appliances and battery.

A. Distributed Voltage Control

One of the key features to be incorporated in our DC microgrid is the distributed control of the grid-voltage. This allows for instantaneous signaling of power available in the source-converter and enables on-the-fly power-sharing between the connected PMUs. Similar techniques have been explored for enabling fast signaling of power-sharing information in DC microgrids [11], [12]. The source-converter allows the voltage to operate in a range between 360-400 VDC and the PMUs have a controllable power-profile (load-line) (Figure 3) based on internal parameters as well as information provided through digital communications.

B. Power Management Unit Architecture

The PMUs are responsible for converting the grid voltage down to the level of household usage (12V) while presenting a controlled positive-impedance (load-line profile) to the grid in order to enable power-sharing between multiple units and maintain grid voltage. The PMUs consist of the following functional blocks:

1) A DC/DC converter that converts the voltage from the 360-400VDC grid distribution level to the 12V household battery level.
2) Integrated scalable battery storage that enables the PMUs to store energy at the households and decouple power-draw from both grid-voltage and local usage, thus enabling the distributed stabilization of grid-voltage.
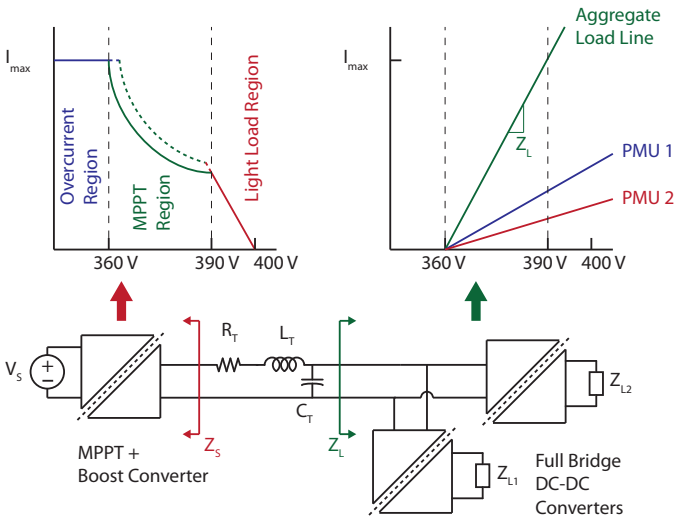3) A communications block that enables sharing of usage information and remote management.

Figure 3. Overview of a grid with two PMUs connected to a single source-converter. The source impedance reflects maximum power available from the solar panels. The aggregate load-lines reflects the aggregate input-impedance of the PMUs as a function of grid-voltage.

IV. THEORY OF OPERATION AND ANALYSIS

In this section, we explore how the design of PMUs and the load-line control scheme ensure stability of the grid voltage in response to disturbances. The steady-state grid-voltage is determined by the aggregate load-line of all the PMUs connected to the grid and the power available from the source converter. A change in load-conditions results in a new grid-voltage operating point as shown in Figure 4. The operating point is determined by the combination of the aggregate load-line and the available power from the source converter. The base topology used for the PMUs is a Phase-shifted full bridge (PSFB) converter (Figure 5). In addition to having a favorable property of magnetic isolation the transformer-isolated PSFB circuit also easily enables zero-voltage switching by utilizing the leakage inductance of the transformer[13].

A. Open-loop response of Phase-Shifted Full-Bridge converter

The Phase-shifted topology is a buck-derived topology and lends itself to analysis by using a PWM buck converter as an analogous circuit. However, the leakage inductance causes the small-signal behavior to diverge from that of a buck converter. The small signal behavior of the PSFB topology has been analyzed in depth by numerous past papers [14], [15]. The impact of the leakage inductance is analogous to current feedback and has a damping effect on the circuit. For the purpose of analysis in this paper we make the simplifying assumption that the variation in current through the output inductor L_{out}, and the variation in voltage across the capacitors C_s and C_{out} are small compared to the nominal values of those quantities over a switching period. This assumption simplifies the analysis of the small-signal model but still accounts for the first-order effects of the leakage inductance. Choosing the current through L_{out} and the voltage across C_s as the state variables the system
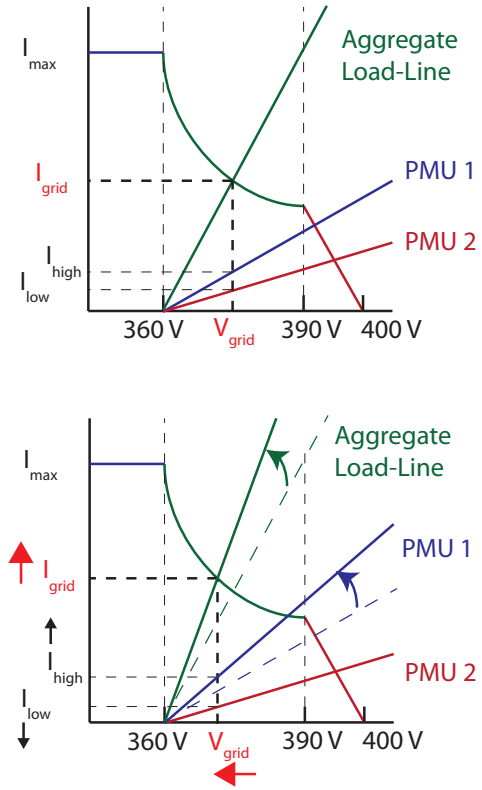

Figure 4. Overview of the response of grid voltage to a change in load conditions. PMU 1 increases the slope of its load-line and changes the set-point of the grid voltage.
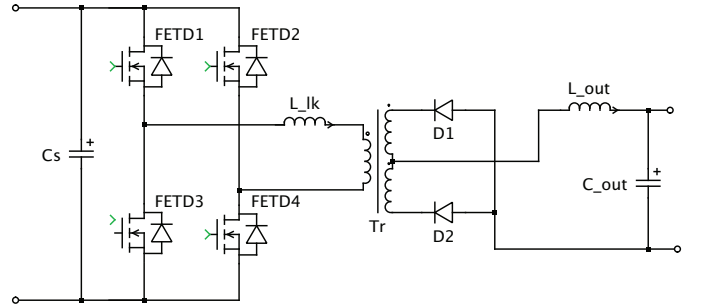

Figure 5. Basic Phase-Shifted Full-Bridge DC-DC converter schematic.

of equations that determine the the operation of the converter are shown to be:

$$L\frac{\mathrm{d}I_l}{\mathrm{dt}} = D_{eff} \cdot \frac{1}{n} \cdot V_c - V_{out} \tag{1}$$

$$C\frac{\mathrm{d}V_c}{\mathrm{dt}} = I_s - D_{eff} \cdot \frac{1}{n} \cdot I_l \tag{2}$$

where I_s is the input current from the grid, n is the turns ratio of the primary windings to the secondary windings of the transformer (n_p/n_s), V_{out} is the battery voltage and hence assumed to be constant, $L = L_{out}$, $C = C_s$, and D_{eff} is the effective duty ratio defined as:

$$D_{eff} = D_{nom} - \Delta D \tag{3}$$

where ΔD is the deviation from the nominal duty cycle caused by leakage inductance commutation, which as mentioned above can be approximated as:

$$\Delta D = \frac{1}{\frac{V_s}{L_{lk}} \cdot \frac{T_s}{2}} \cdot 2 \cdot \frac{I_l}{n} = \frac{R_l}{V_s} \cdot I_l \qquad (4)$$

where $R_l = 4 \cdot L_{lk}/T_s$.

Solving for the steady-state operating point of the converter we get that:

$$I_l = \frac{I_s \cdot V_{out} \cdot n}{D_{nom} \cdot V_{out} - I_s \cdot R_l} \qquad (5)$$

$$V_c = \frac{V_{out}^2 \cdot n}{D_{nom} \cdot V_{out} - I_s \cdot R_l} \qquad (6)$$

Figure 6 shows the open-loop characteristic of the steady-state grid voltage as a function of grid current. The current-feedback effect caused by the leakage inductance makes the effective impedance of the PMU on the grid always positive. Additional feedback can enhance (or modify) this characteristic this will be shown below.

The small-signal perturbation state-space model can be derived from the large-signal equations (1-4) above and it takes the form:

$$\dot{x} = A \cdot x + b_1 \cdot \hat{d} + b_2 \cdot \hat{i}_s + b_3 \cdot \hat{v_{out}} \qquad (7)$$

where $x = [\begin{array}{cc} \hat{i}_l & \hat{v}_c \end{array}]^t$ and all system variables: $[\begin{array}{ccccc} \hat{i}_l & \hat{v}_c & \hat{d} & \hat{i}_s & \hat{v}_{out} \end{array}]$, are perturbations from nominal operating points. The relevant matrices of the system are:

$$A = \left[\begin{array}{cc} -R_l/L \cdot n^2 & -D_{nom}/L \cdot n \\ -D_{nom}/C \cdot n & -R_l \cdot I_l^2/C \cdot n \cdot V_c^2 \end{array}\right]$$

$$b_1 = \left[\begin{array}{c} V_c/(n \cdot L) \\ -I_l/(n \cdot C) \end{array}\right]$$

$$b_2 = \left[\begin{array}{c} 0 \\ 1/C \end{array}\right]$$

$$b_3 = \left[\begin{array}{c} -1/L \\ 0 \end{array}\right]$$

We can derive transfer functions and impedance functions for the converter from (7). An example of the small-signal response of the grid-capacitor voltage ($\hat{v}_c$) to a change in the duty cycle is shown in Figure 7. The leakage inductance has a damping effect on the response of $\hat{v}_c$ in comparison to a conventional Buck converter. The open-loop input impedance (i.e. response of $\hat{v}_c$ to $\hat{i}_s$) shown in Figure 8 also highlights the damping effect due to L_{lk} in the PSFB converter. This characteristic opens up the possibility of utilizing network passivity concepts [16] to make an argument for large-scale grid stability of multiple-interconnected PMUs.
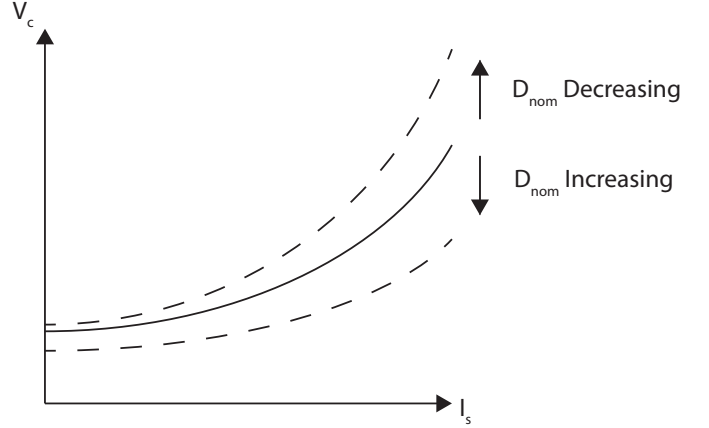

Figure 6. Open-loop steady-state response of grid-capacitor voltage to input current drawn by a phase-shifted full bridge converter.
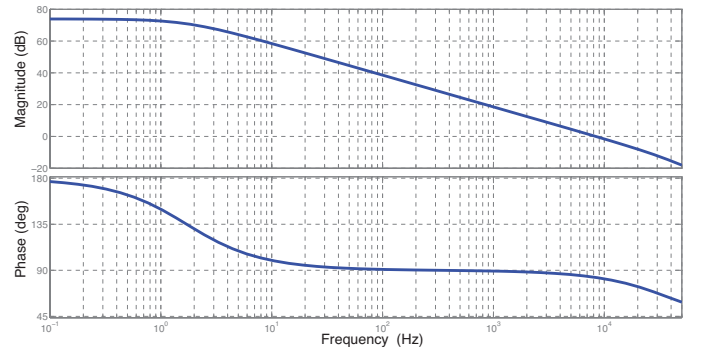

Figure 7. Control-to-grid capacitor voltage transfer function ($\hat{v}_c(s)/\hat{d}(s)$) of the PS-full bridge converter.

B. Closed-Loop Response of Phase-Shifted Full-Bridge Converter

As explained in Section III, the desired control objective of the PMUs is to present a load-line profile to the grid, i.e. the PMUs should behave as controllable positive impedances to stabilize the grid voltage to a unique operating point under each set of source & load conditions. The choice of PS-full bridge converter topology has the favorable properties
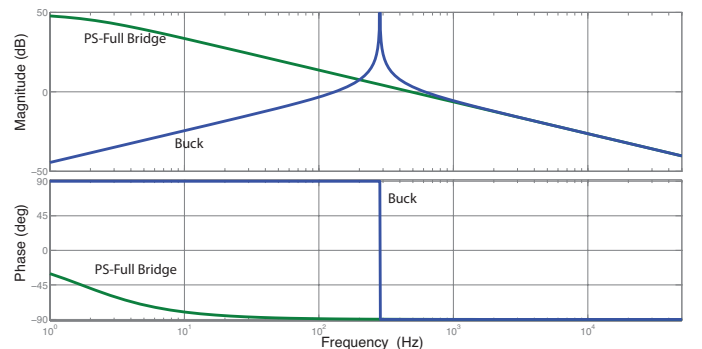

Figure 8. Open-loop input-impedance ($\hat{v}_c(s)/\hat{i}_s(s)$) of the PS-full bridge converter as compared to a conventional Buck converter.
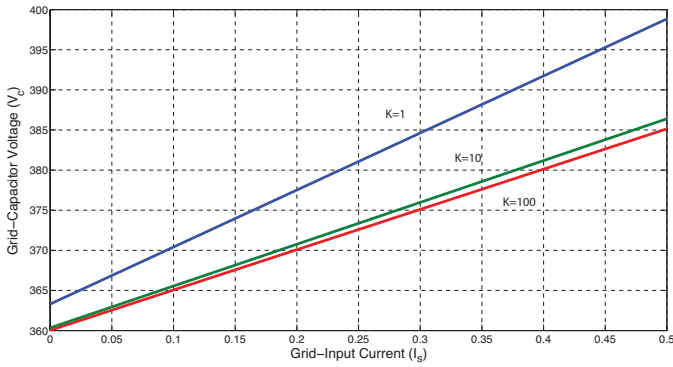
Figure 9. Steady-state, closed-loop response of the grid-capacitor voltage (V_c) to the input current (I_s) of the PS-full bridge converter for increasing feedback gain.

Figure 10. Steady-state, closed-loop input-conductance of the PS-full bridge converter as a function of input-current (I_s) for increasing feedback gain.

of both large-scale and incremental passivity under open-loop operation; such converters have been shown to be stable using an energy-conservation (Lyapunov) based arguments [16]. The desired load-line controller would enforce the following relationship between the input current (I_s) and the grid-capacitor voltage (V_c):

$$I_s = G_{desired}(V_c - V_{ref}) \qquad (8)$$

where $G_{desired}$ is the desired slope of the load-line and V_{ref} is the cut-off grid-voltage as shown in Figures 3 & 4.

It is possible regulate the slope of the load-line of an individual PMU through simple proportional feedback:

$$D = -K_p \cdot [I_s - G_{desired}(V_c - V_{ref})] \qquad (9)$$

where K_p is the proportional feedback gain. Following through with a similar analysis to the previous section, the steady-state grid-capacitor voltage (V_c) response to input-current (I_s) of a PMU is shown in Figure 9, with $G_{desired} = 0.02$ and $V_{ref} = 360$V. The desired load-line behavior is achievable even with a low values of feedback gain $(K_p{=}10)$. We can see from Figure 10 that while there is a steady-state error in G_{actual} (input conductance) for lower values of K_p, the conductance stays constant across the range of input-current values.

The small-signal input-impedance function $(\hat{v}_c(s)/\hat{i}_s(s))$ can be derived by solving 7 and using the following small-signal approximation for $\hat{d}(s)$:

$$\hat{d}(s) = -K_p(\hat{i}_s(s) - G_{desired} \cdot \hat{v}_c(s)) \qquad (10)$$

Figure 11 highlights the damping effect of leakage inductance on the closed-loop input-impedance for $K_p = 10$. As described previously in Section IV-A, this damping characteristic along with the load-line feedback control scheme open up the possibility of utilizing network passivity concepts [16] for justifying global stability of a larger networked grid-system with multiple independently operating PMUs regulating the grid-voltage over the full-range of operating conditions.
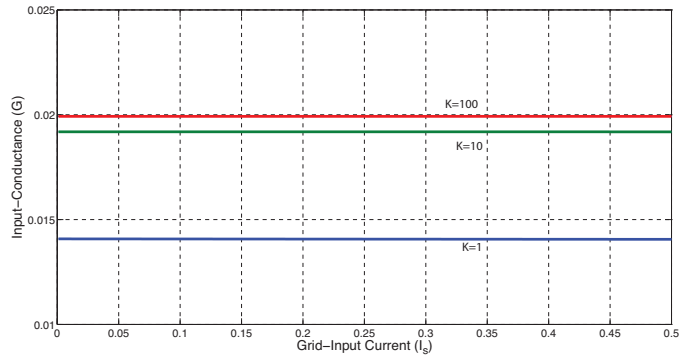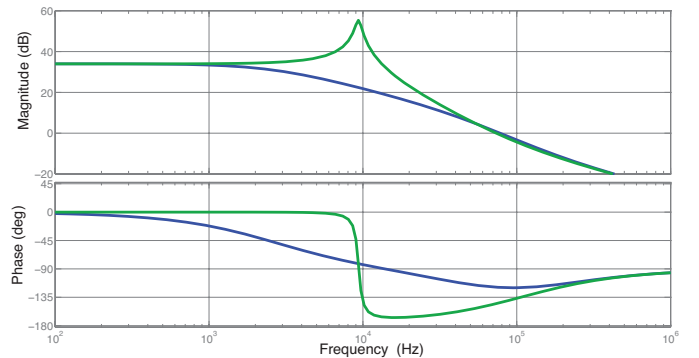

Figure 11. Closed-loop, small-signal input-impedance $(\hat{v}_c(s)/\hat{i}_s(s))$ of the PS-full bridge converter as compared to a conventional Buck converter. A proportional feedback of the load-line variable: $D = -K_p(I_s - G_{desired}(V - V_{ref}))$ with $Kp = 10$ is used in both cases.

V. SIMULATION RESULTS

In this section results obtained using the PLECS simulation toolset are used to verify grid-voltage stability. The simulation setup is shown in Figure 12. A simple topology of 2 PMUs connected to a constant power source is used for the simulations presented in this section. The constant power source is realized as a dependent current source whose output is dependent on the voltage across its terminals, i.e. $I_{grid} = P/V_{grid}$.

Figure 13 shows the response of grid voltage as there is a step change in input power from 100W-150W. Each PMU draws an equal amount of power since they are both regulating to the same slope $(G_{desired})$ and have the same feedback gain (K_p). The grid-voltage stabilizes to a new steady-state solution after a transient period and the response of grid voltage exhibits a damped behavior that is in agreement with the analysis carried out in the previous section. The PMUs both increase their power draw in response to rising grid-voltage. This behavior ensures stability of the grid-voltage under changing power-conditions.

VI. EXPERIMENTAL PLAN

Experimental verification of the distributed voltage control scheme is currently being carried out by programming com-
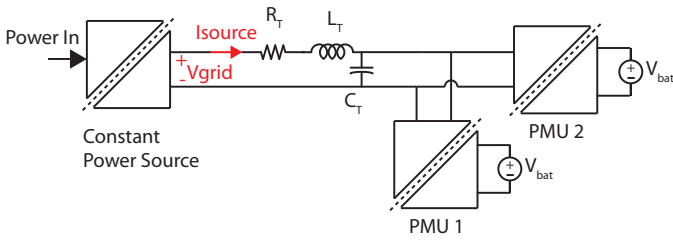
Figure 12. Simulation setup used in PLECS with a single constant-power source connected to two PMUs. $R_T = 0.1\Omega$, $L_T = 10\mu H$, and $C_T = 30\mu F$ are the transmission-line parameters.
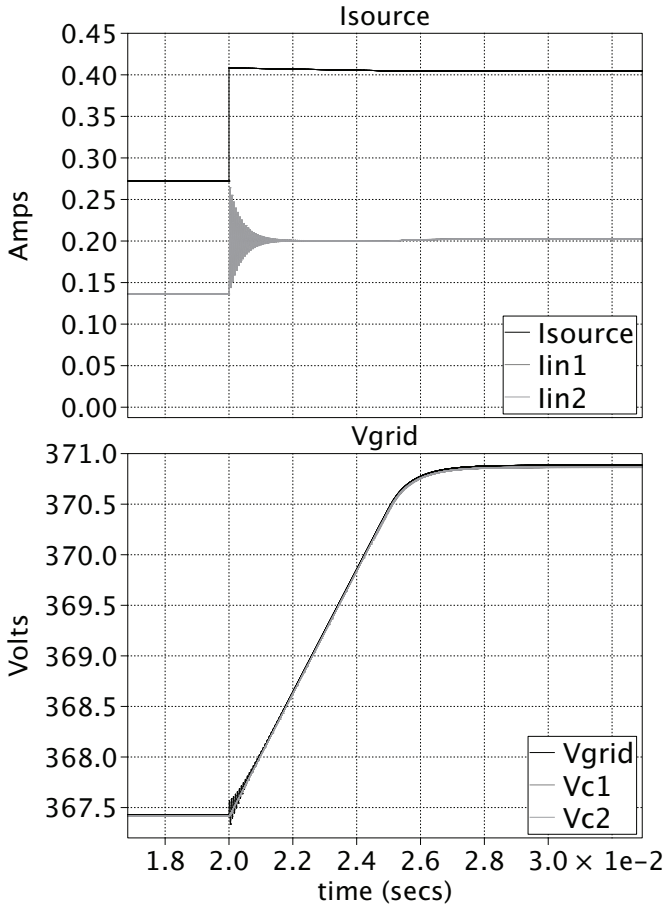

Figure 13. Simulated response of grid-voltage to a step change in input power from 100W-150W.

mercially available (Texas Instruments) Phase-Shifted Full-Bridge converters to function as the PMUs. We have built a prototype system to observe the behavior of the various components in response to disturbances. The power source of the system is the peak-power-tracked output of a 400W solar panel installation. We will connect the MPPT-source to multiple independently operating PMUs to replicate the setup in Figure 12. Experimental results will record the behavior of the grid-voltage in the presence of varying input power as well as changes in the commanded load-lines slopes of the connected PMUs. Experiments will also be conducted to

ensure stable operation in case of faults: both where a short occurs, and where all loads are simultaneously taken offline.

VII. CONCLUSIONS

DC microgrids are an effective means of achieving the efficiency gains needed to make rural microgrids cost-effective. This paper presents the analytical justification for using a distributed voltage-control scheme to stabilize the grid-voltage under a wide-range of operating conditions. Our simulations of a simple system with 2 PMUs connected to a power-source show the stability of the proposed microgrid under a power transient. Development of the individual components of the microgrid system and the planned experiments described above will be used to show the stability of the microgrid under normal operation as well as in recovery from faults.

The next step for our research group is to prototype a full-scale system with ~20 PMUs connected to a larger generation source to obtain experimental verification of the stability and efficiency-gains of a realistically sized DC village-grid system. A field-ready version DC microgrid system will be deployed in the Philippines early next year. We will verify the overall system-efficiency and cost-savings that we have predicted with using a DC system. We also seek to use field studies to show that providing reliable electricity encourages adoption of energy efficient devices. After testing, another round of impact analysis will be performed to inform the next microgrid design.

ACKNOWLEDGMENT

REFERENCES

[1] "ENERGY FOR ALL: Financing access for the poor," *IEA World Energy Outlook 2011*, Sep. 2011.
[2] M. Nouni, S. Mullick, and T. Kandpal, "Providing electricity access to remote areas in India: An approach towards identifying potential areas for decentralized electricity supply," *Renewable & Sustainable Energy Reviews*, vol. 12, no. 5, pp. 1187–1220, Jun. 2008.
[3] L. Srivastava and I. H. Rehman, "Energy for sustainable development in India: Linkages and strategic direction," *Energy Policy*, vol. 34, no. 5, pp. 643–654, Mar. 2006.
[4] D. Soto, E. Adkins, M. Basinger, and R. Menon, "A prepaid architecture for solar electricity delivery in rural areas," in *Proceedings of the Fifth International Conference on Information and Communication Technologies and Development. ACM*, 2012, pp. 130–138.
[5] D. Boroyevich, I. Cvetkovic, D. Dong, R. Burgos, F. Wang, and F. Lee, "Future electronic power distribution systems a contemplative view," *Optimization of Electrical and Electronic Equipment (OPTIM), 2010 12th International Conference on*, pp. 1369–1380, 2010.
[6] W. Zhang, D. Dong, I. Cvetkovic, F. Lee, and D. Boroyevich, "Lithium-based energy storage management for DC distributed renewable energy system," *Energy Conversion Congress and Exposition (ECCE), 2011 IEEE*, pp. 3270–3277, 2011.
[7] D. Soto and V. Modi, "Simulations of Efficiency Improvements Using Measured Microgrid Data," *Global Humanitarian Technology Conference (IGHTC), 2012 IEEE*, pp. 369–374, 2012.
[8] W. Stevens and G. P. Corey, "A study of lead-acid battery efficiency near top-of-charge and the impact on pv system design," *Photovoltaic Specialists Conference, 1996., Conference Record of the Twenty Fifth IEEE*, pp. 1485–1488, 1996.

[9] A. C. Brent and D. E. Rogers, "Renewable rural electrification: Sustainability assessment of mini-hybrid off-grid technological systems in the African context," *Renewable Energy*, vol. 35, no. 1, pp. 257–265, Jan. 2010.

[10] "Power supplies: A hidden opportunity for energy savings," *A NRDC report prepared for Natural Resources Defense Council, San Francisco, CA*, 2002.

[11] L. Zhang, T. Wu, Y. Xing, K. Sun, and J. M. Gurrero, "Power control of DC microgrid using DC bus signaling," *Applied Power Electronics Conference and Exposition (APEC), 2011 Twenty-Sixth Annual IEEE*, pp. 1926–1932, Nov. 2010.

[12] W. Jiang and Y. Zhang, "Load Sharing Techniques in Hybrid Power Systems for DC Micro-Grids," *Power and Energy Engineering Conference (APPEEC), 2011 Asia-Pacific*, pp. 1–4, 2011.

[13] J. A. Sabate, V. Vlatkovic, R. Ridley, F. Lee, and B. H. Cho, "Design considerations for high-voltage high-power full-bridge zero-voltage-switched PWM converter," in *Applied Power Electronics Conference and Exposition, 1990. APEC '90, Conference Proceedings 1990., Fifth Annual*, 1990, pp. 275–284.

[14] V. Vlatkovic, J. A. Sabate, R. Ridley, F. Lee, and B. H. Cho, "Small-signal analysis of the phase-shifted PWM converter," *Power Electronics, IEEE Transactions on*, vol. 7, no. 1, pp. 128–135, 1992.

[15] M. J. Schutten and D. A. Torrey, "Improved small-signal analysis for the phase-shifted PWM power converter," *Power Electronics, IEEE Transactions on*, vol. 18, no. 2, pp. 659–669, Mar. 2003.

[16] S. Sanders and G. C. Verghese, "Lyapunov-based control for switched power converters," *Power Electronics, IEEE Transactions on*, vol. 7, no. 1, pp. 17–24, 1992.